Mitigating Risks at Bus Stops: A Study of the Effectiveness of Bollard Systems

Jonathan Lazatin [1], Pouya Shojaei, Ph.D.[2], Brendan O'Toole, Ph.D.[1], Mohamed Trabia, Ph.D.[1],

[1] Department of Mechanical Engineering, University of Nevada, Las Vegas, 4505 South Maryland Parkway, Las Vegas, NV 89154, USA

[2] ANSYS, 2600 Ansys Dr. Canonsburg, PA, 15317, USA

1. Abstract

This work assesses the effectiveness of a proposed interconnected multi-bollard design in protecting bus stop occupants from incoming vehicles. A detailed model of a 3-bollard system was developed in ANSYS LS-Dyna®, which included the bollards, their underground support structures, and the rebars connecting the bollards. The bollard system was composed of 116 parts with a total of 443,799 elements. The system model was merged with a detailed model of a 2007 Chevrolet Silverado, 4-door crew cab pickup truck with 603 parts with 251,400 elements developed by the Center for Collision Safety and Analysis [1]. The vehicle was simulated to impact the bollard system at speeds between 15 and 90 mph at angles ranging from 0° (normal to the bollard system) and 90° (parallel to the bollard system). Impacts were also made at various degrees of centeredness, with cases showing response from impact at the center of bumper, as well as at the edge of the bumper. With each case, vehicle velocity and acceleration were monitored using virtual accelerometers, placed in the vehicle to assess the effectiveness of the bollard to stop the vehicle. Simulation results show that the bollard was able to stop a vehicle traveling normal to the bollard system, impacting the center of the bumper at speeds up to 45 mph. However, the vehicle would continue past the bollard system at higher speeds.

2. Introduction

The Regional Transportation Commission (RTC) of Southern Nevada manages the public transit services across the Las Vegas Metropolitan area. RTC's Fixed route public transit services consist of 38 routes that serve the region's residents and visitors. These routes include about 3,300 transit stops, and they served more than 35 million passenger trips in FY 2021, including 273,000 riders with wheelchairs and 439,000 bicycles transported [2]. The safety of riders is critically important to the RTC including the safety of those at transit stops. While RTC's overall safety record has been very good, each year, a few of its stops have been struck by motor vehicles. Fortunately, the majority of such incidents have not resulted in significant harm to transit patrons or others in the proximity of transit stops.

Figure 1. A possible layout of bollards at a bus stop at a major intersection [3].

RTC is taking proactive measures to mitigate those risks. Figure 1 shows one of many potential locations currently under consideration for the integration of protective bollard systems. As shown in Figure 2, the proposed bollard solutions include a shallow mount bollard system that extend 48” above the concrete and are placed 12” below concrete. The cylindrical body of the bollard is made of a 10” schedule 60 A500, Grade B steel pipe with a welded 1.5” A36 Steel stiffener plate.

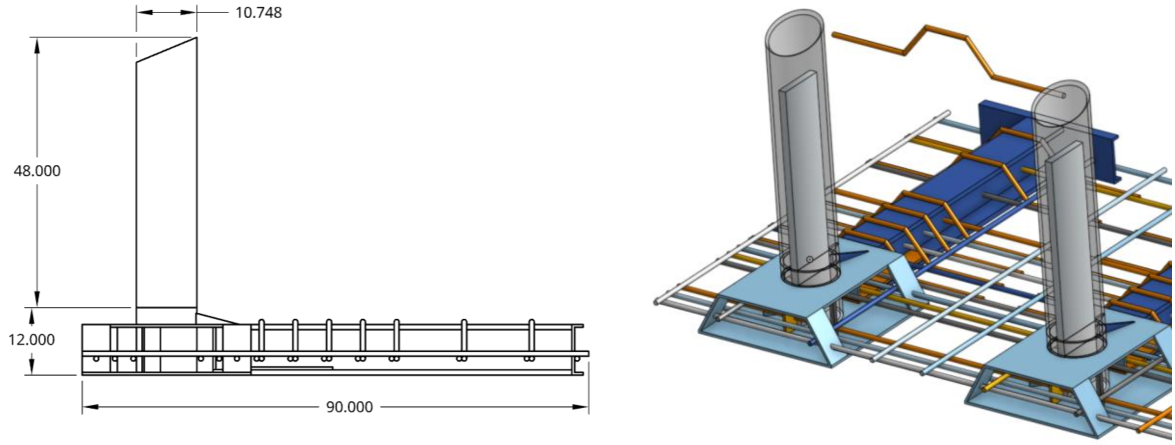

Figure 2. Bollard model diagram showing interior stiffener bar, cylindrical body, Lower mounting structure, and rebar matrix highlighting bent rebar component.

The bollard is mounted into a half inch thick steel plate trapezoidal box structure with a W8X67 W-Beam extending backwards to a C channel. Holes are placed through the beams to allow for the rebar matrix to pass through. The rebar matrix utilizes #7 size rebar with 14 horizontal rebar segments connecting each bollard, with four vertical rebar posts per bollard. A bent rebar section is placed over the W beam and paired with a horizontal rebar section. Figure **3** shows a model of the three bollards, their support structures, and the rebars connecting them.

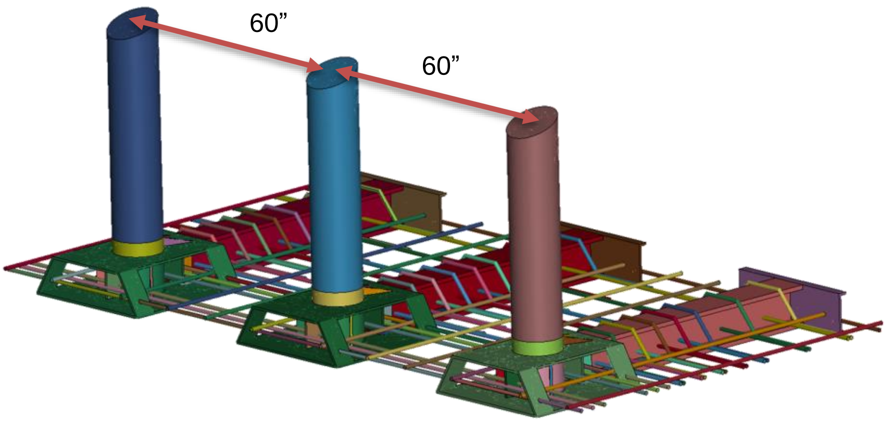

Figure 3**. Three-bollard system with supporting rebars.**

The main objective of this research is to assess the effectiveness of the proposed bollard design for the protection of the occupants of a bus stop from death and injury due to car impact. Using the current planning documents to configure bollard structures, an analysis was conducted to determine the efficacy of such systems in stopping oncoming vehicles, and the potential effect on the driver. By simulating cases where the vehicle impacts a bollard system at various speeds, angles, and positions, a complete understanding of the effectiveness of the bollard system in stopping vehicles can be reached.

3. Model Development

A finite element model (FEM) of a 2007 Chevrolet Silverado 4-door crew cab pickup truck was used. This model was developed by the Center for Collision Safety and Analysis (CCSA) at George Mason University using LS-Dyna software [1]. For this study, the rigid wall was removed and replaced with the three-bollard system of Figure 4. Details of the truck model are shown in Table 1.

Table 1. Model details for 2007 Silverado from Center for Collision Safety and Analysis (CCSA, 2016).

Vehicle Model Details	
Number of Parts	603
Number of Nodes	262,061
Number of Solid Elements	12,517
Number of Shell Elements	236,352
Number of Beam Element	2,531
Total Elements	251,400

Figure 4. FEA model of 2007 Silverado, course mesh (CCSA, 2016).

The 3-bollard system model with underground support structure, beams, and rebar was imported as a SLDPRT file to ANSYS Space Claim as two primary geometries. First the Bollard, W beam, and C channel components were imported, and the geometry was edited to ensure shared faces and edges generated shared nodes. This geometry was copied to generate 3 instances in the final ANSYS Mechanical model. The rebar matrix was imported as a separate geometry.

The geometries were assembled in ANSYS Mechanical for defining contacts and boundary conditions. Fixed boundary constraints were used on the bottom surfaces of each of the ends of the rebar as shown in Figure 5. The various parts of the bollard structure were defined with bonded contact regions. This contact definition was included at each interface of the underground structure, including the mounting box, stiffening flanges, and connective beams. Figure 6 shows the contact faces where the W-beam meets the C-channel.

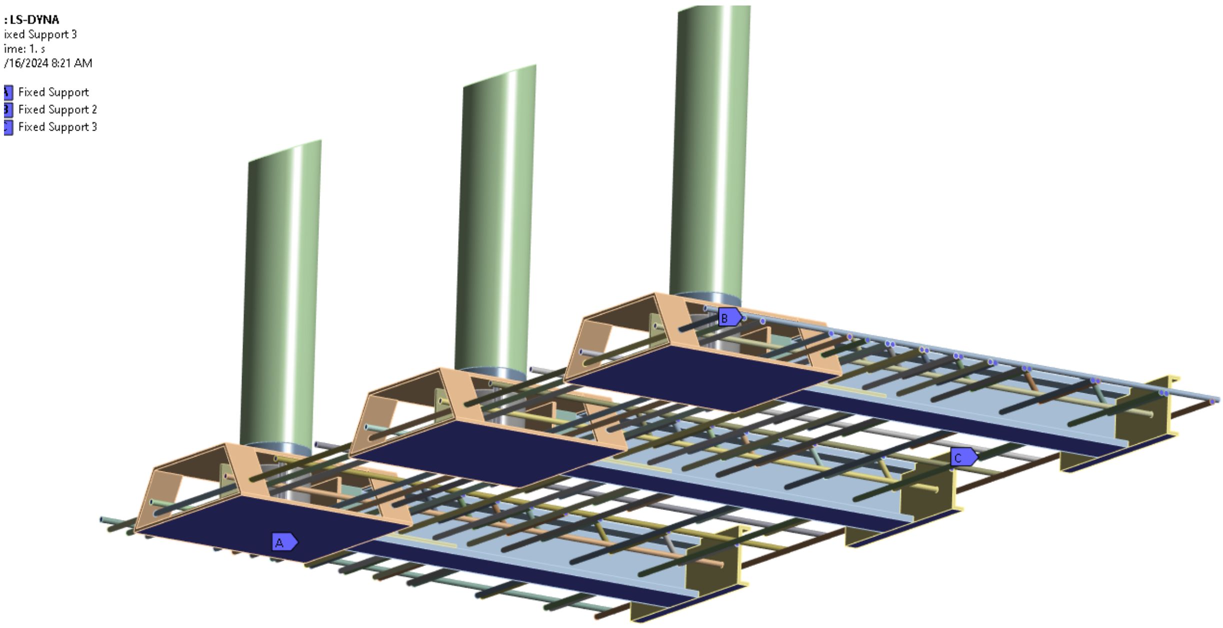

Figure 5. Fixed supports placed on bottom surface of bollard mounting structure and end of rebars.

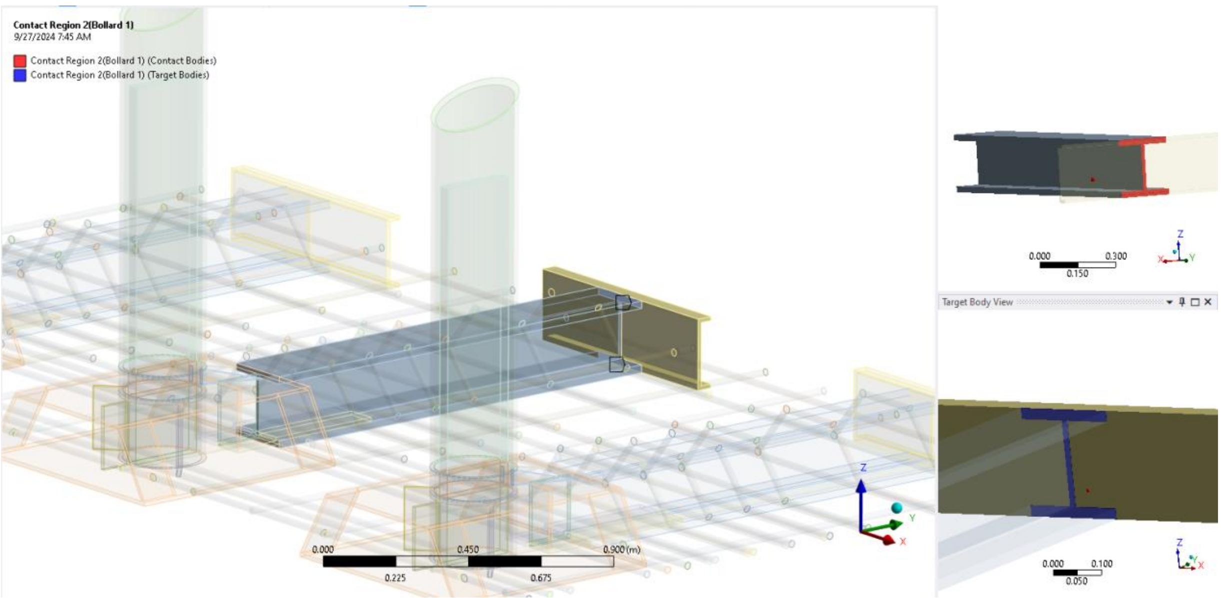

Figure 6. Example bollard body contact definition where W-beam meets the C-channel.

The rebar matrix was also modeled with bonded contacts at each interface with another rebar, and each contact point with the bollard mounting structure. Figure 7 shows various bonded contacts including between two rebars, rebar to a W-beam, and rebar to the mounting box. The mesh, shown in Figure 8, was also created in ANSYS Mechanical and exported as a keyword file for use in LS-Dyna for simulation.

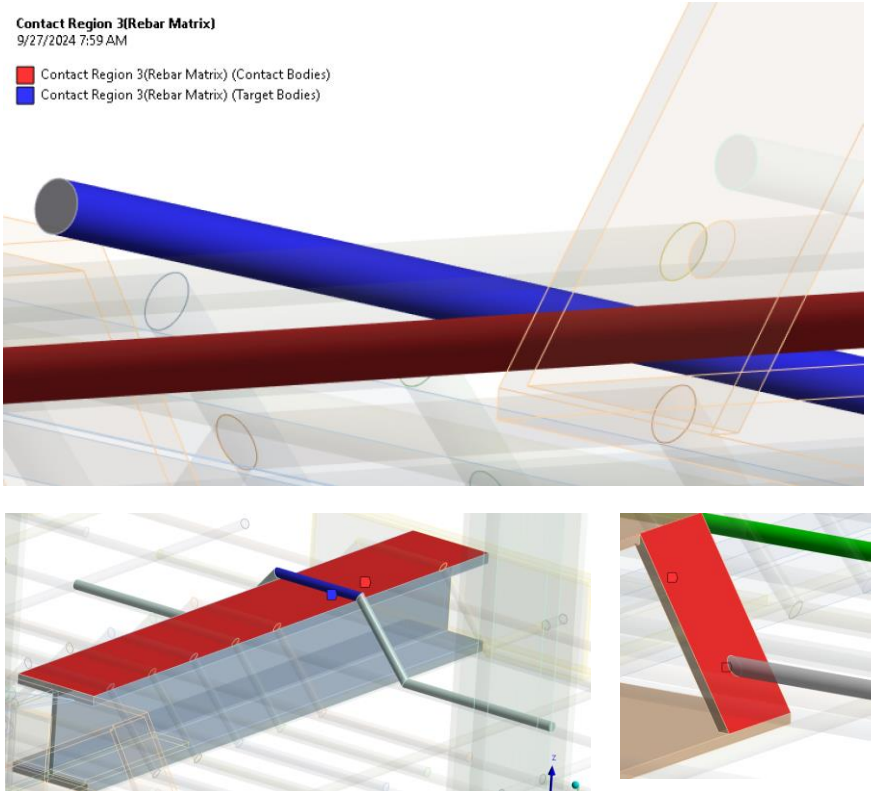

Figure 7. Bonded contacts at the interfaces including rebar to rebar, rebar to box W-beam, and rebar to mounting box structure.

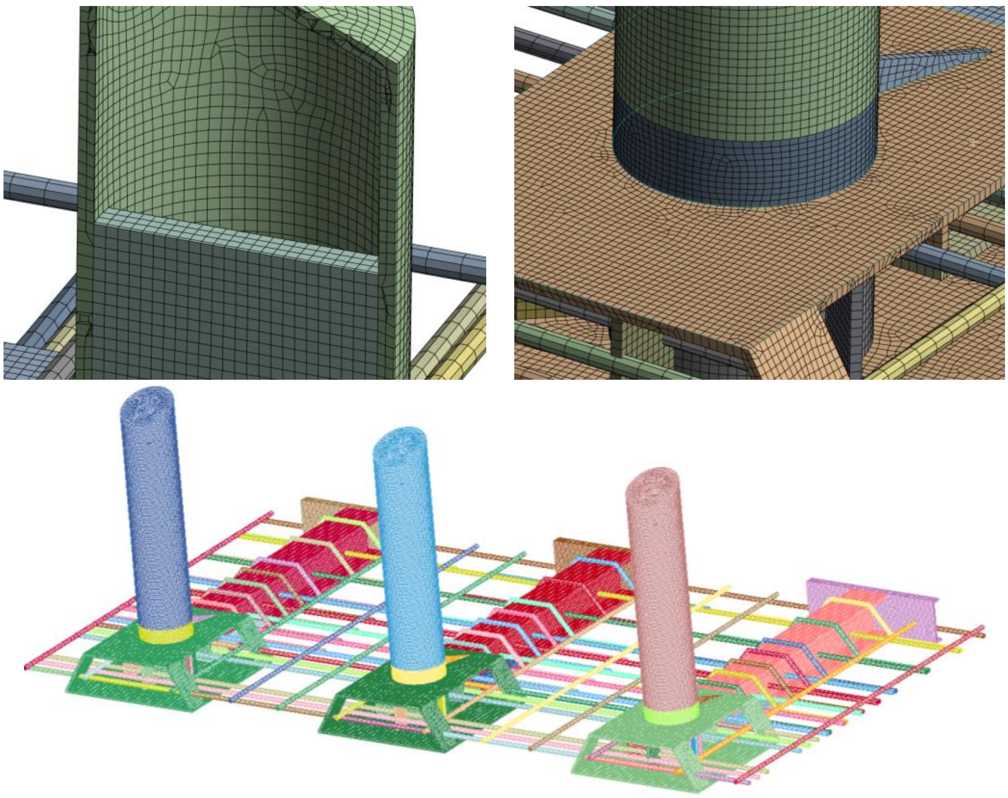

Figure 8. 3D model and mesh of the 3-bollard system.

The bollard keyword file was combined with the truck simulation file, replacing the rigid wall object. Information about the bollard model is shown in Table 2 below. Material properties were added to the model using LS-Dyna material keywords. The material for the bollard system was modeled using a linear piecewise material keyword. The exterior cylindrical body of the bollard was model as A5000 Grade B Steel and the interior Stiffener Bar was modeled after ASTM A36 steel, per shop drawing specifications. The mounting box, I-Beam structure, and rebar matrix were also modeled using the same A36 steel material properties keyword as the stiffener.

Table 2. Bollard System Model Details.

3 Bollard System Model	
Parts	116
Nodes	495,367
Elements	443,799

4. Parametric Study Setup

A parametric study was conducted simulating the vehicle impacting the bollard system at different speeds, angles, and impact positions as indicated in Figure 9. The vehicle model was set with an initial velocity, and the bollard system was placed at varying angles and positions to induce the desired impact position. The positions included a centered on the bumper, to a shift of a quarter bumper width, and an impact at the corner of the bumper (a half bumper width). The vehicle angle was also modified and included impacts at 0° (normal to the bollard system), 30°, 45°, 60°, and 90° (parallel to bollard system). Impact velocities were also swept from 15, 30, 60, and 90 mph.

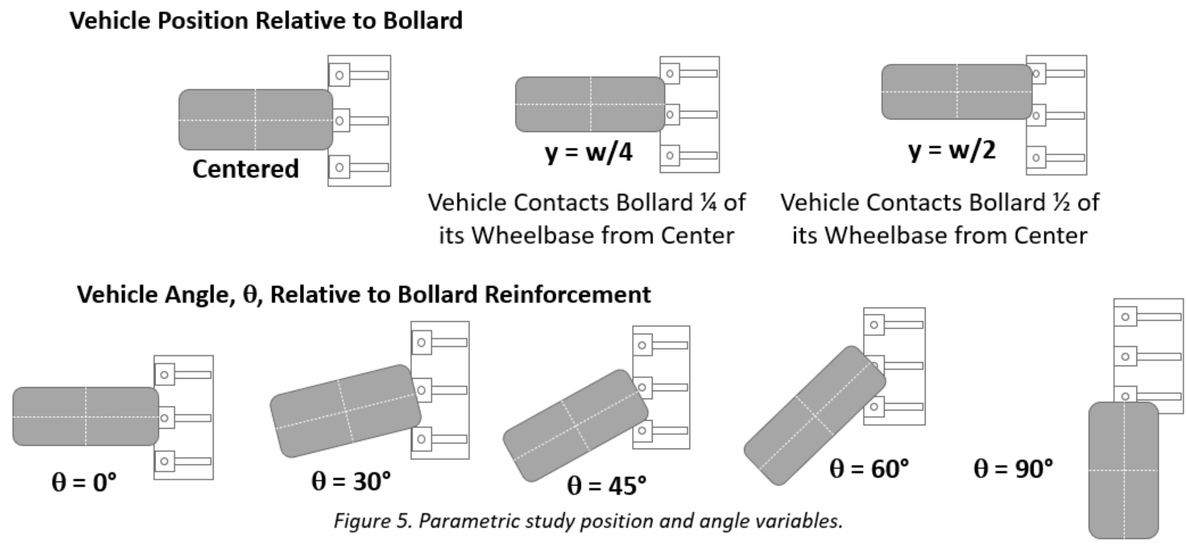

Figure 9. Parametric study variables for initial conditions.

5. Results

A subset of results is presented here, showing some of the key findings and relationship between the bollard impact condition and the effectiveness of the system to limit forward progression of the vehicle. Figure 10 shows an image of the vehicle model and its deformation upon contacting the bollard system. Much of the results focus on the x-direction motion, taken as node outputs from a virtual accelerometer placed in the left-rear floor of the cabin, as it is closest to the driver position. The x-axis refers to the axis of initial vehicle travel, as the interest centered around the bollard’s ability to stop forward progression of the vehicle. As many of the major roadways in the RTC area have a speed limit of 45 mph, a centerline impact simulation was conducted with a sweep of impact angles from 0° to 90°.

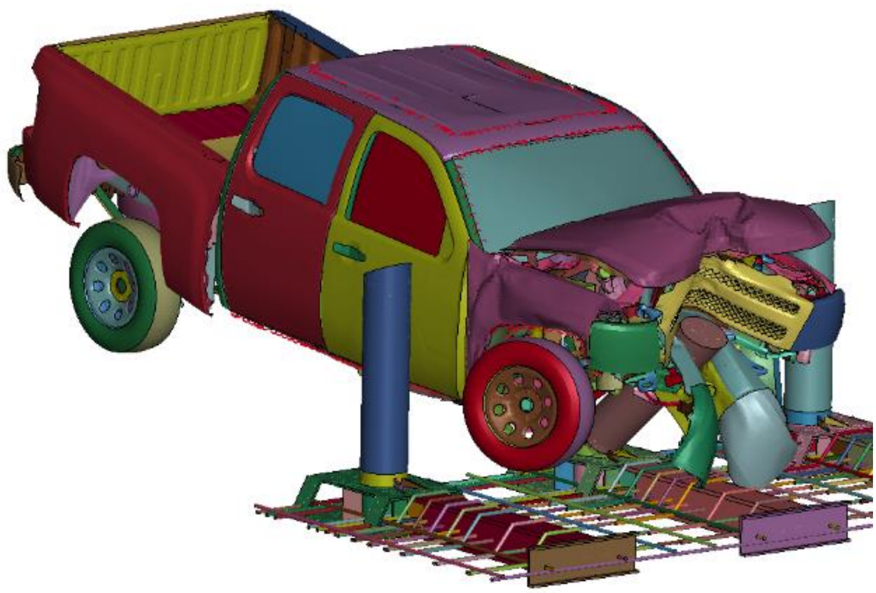

Figure 10. Image of truck collision with bollard system with impact angle of 0 at 45 mph.

The results shown in Figure 11 indicate that up to the 45° point, the bollard system was successfully able to stop the vehicle, with the vehicle reaching 0 mph within 0.25 seconds of impact. At 60° and 90°, however, the vehicle lost most of its velocity but was still able to move a significant distance past the initial bollard impact position. In the 60° case, the bollard eventually stopped, shown in Figure 14, as the vehicle interacted with the subsequent bollard in the system. Figure 12 and Figure 13 indicate that the acceleration in the x-direction slightly decreases in magnitude as angle increases. At higher angles, the stiffener plate inside the bollard becomes less effective and it is suspected that the bollard deforming more as angle increases causes the reduction in the peak acceleration.

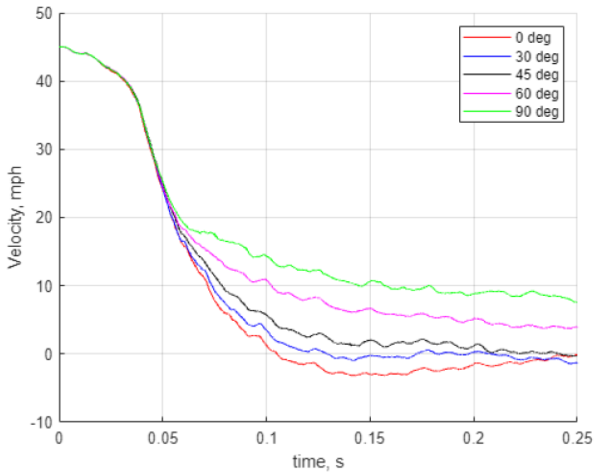

Figure 11. Velocity loss in the x-direction of centered impact at 45 mph swept from 0° to 90°.

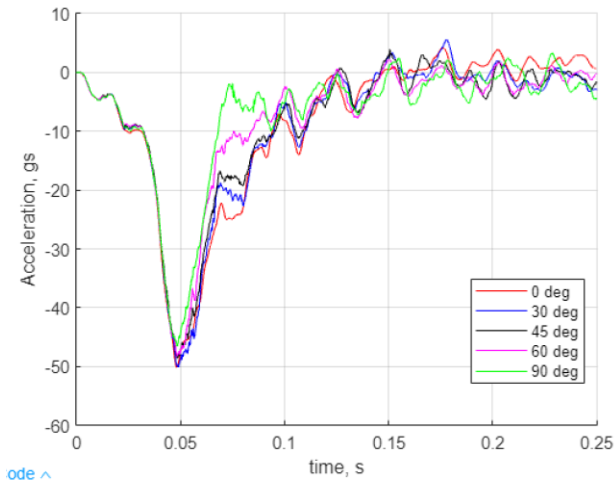

Figure 12. Acceleration in x-direction of centered impact at 45 mph swept from 0° to 90°.

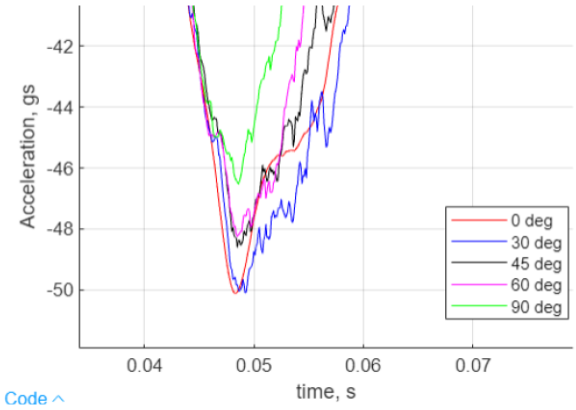

Figure 13. Close up of peak acceleration in the x-direction at 45mph swept from 0° to 90°.

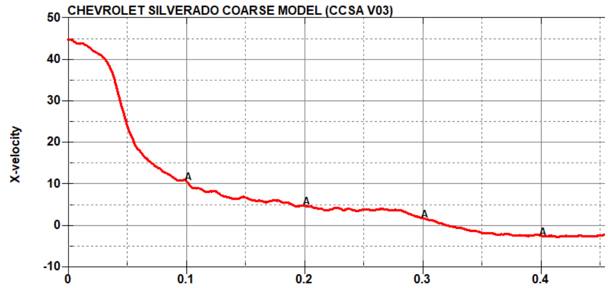

Figure 14. Center impact at 45mph 60° case reaching 0mph and contacting second bollard.

The 45 mph at 0° condition was also simulated with varying impact positions from centered, to quarter bumper shift, to end of bumper. As shown in Figure 15 and Figure 16, the velocity reaches 0 in all cases, with the quarter, and half bumper length shifts actually stopping faster, as the off center collisions force the vehicle to impact more than one bollard within the system.

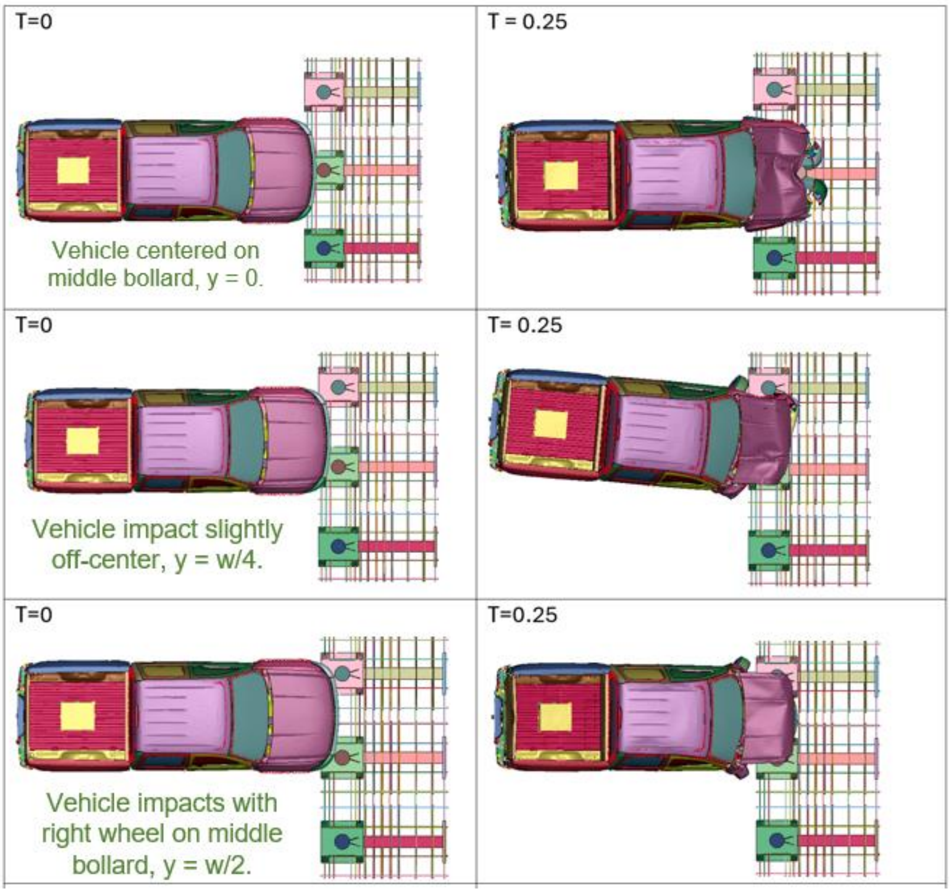

Figure 15. Pre-crash and post-crash images of 45mph 0° case at varying positions.

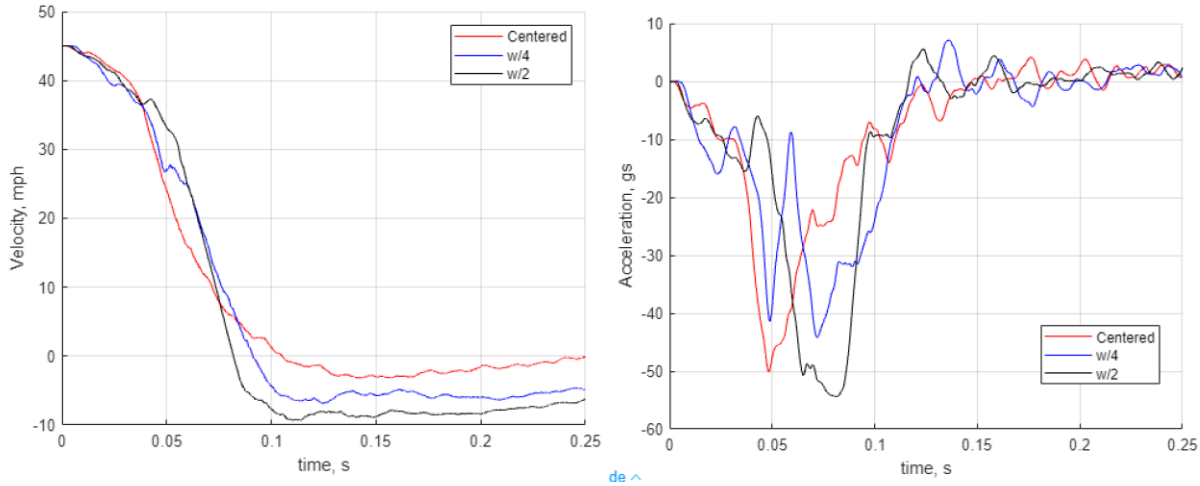

Figure 16. Velocity and acceleration graphs of 45mph 0° cases.

The 30º at 45mph condition was also simulated with varying position along the bumper, shown in Figure 17. The off-center cases again show a faster elimination of the velocity in the x direction, indicated in Figure 18. The center case, however, has the highest peak acceleration, as the other cases dissipate some of the impact energy while causing the vehicle to rotate.

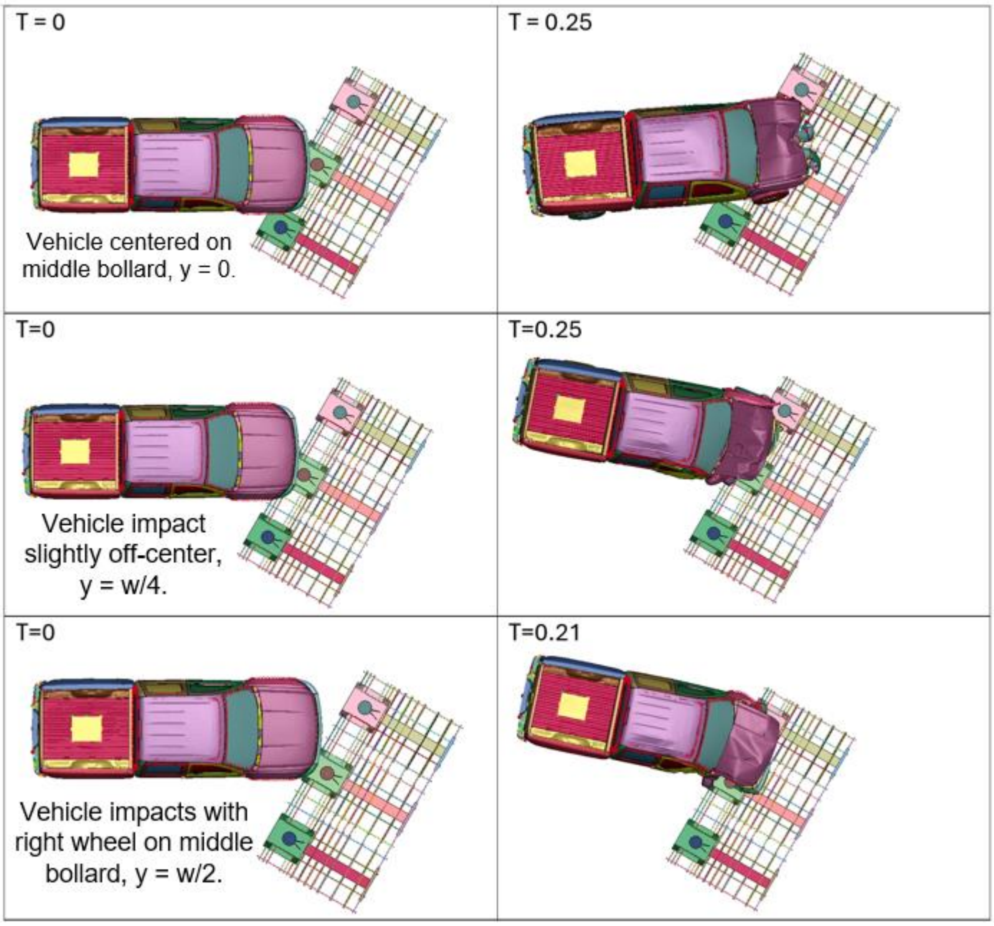

Figure 17. Pre-crash and post-crash images of 45 mph 30° case at varying positions.

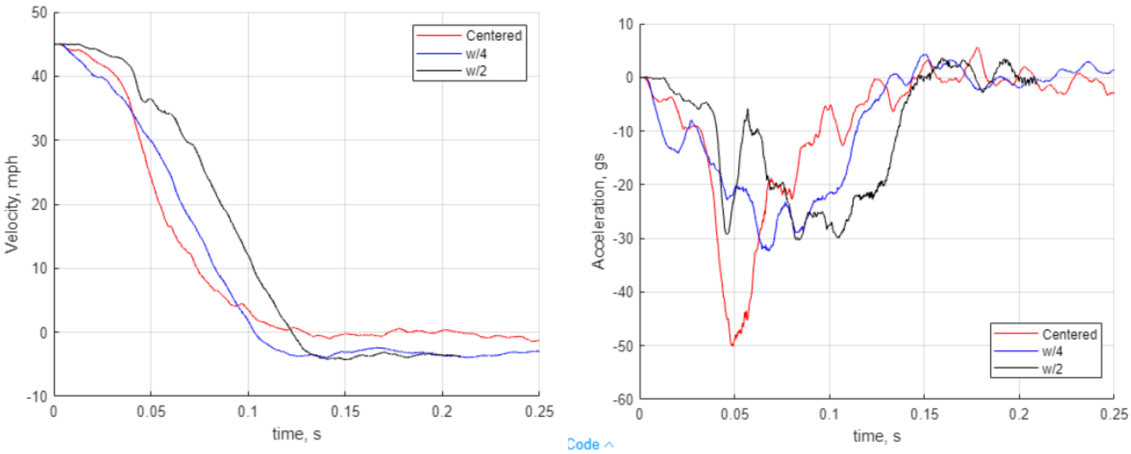

Figure 18. Velocity and acceleration graphs of 45mph 30° cases.

It was generally seen that the more off centered the vehicle impacted the bollard system, the initial drop in velocity is slower. However, once the vehicle contacted a second bollard, the off-center cases reached an x-velocity of 0 mph faster. In these cases, where the vehicle contacts the second bollard, the peak x-acceleration also increases.

The impact of vehicle velocity was also considered for cases ranging from 15 – 90 MPH. Figure 19 shows pre-crash and post-crash images for a 0.25s simulation time. At 60 MPH or higher, the vehicle does not stop within 0.25 seconds and is sown to penetrate deep into the bollard area. Higher speeds induce higher accelerations upon impact. The leveling off the velocity curve shown in Figure 20 indicates that the vehicle would not stop within a reasonable distance in the case of a bollard system being implemented at a bus stop at these speeds. Figure 20 also shows that the higher the speed, the greater the peak acceleration.

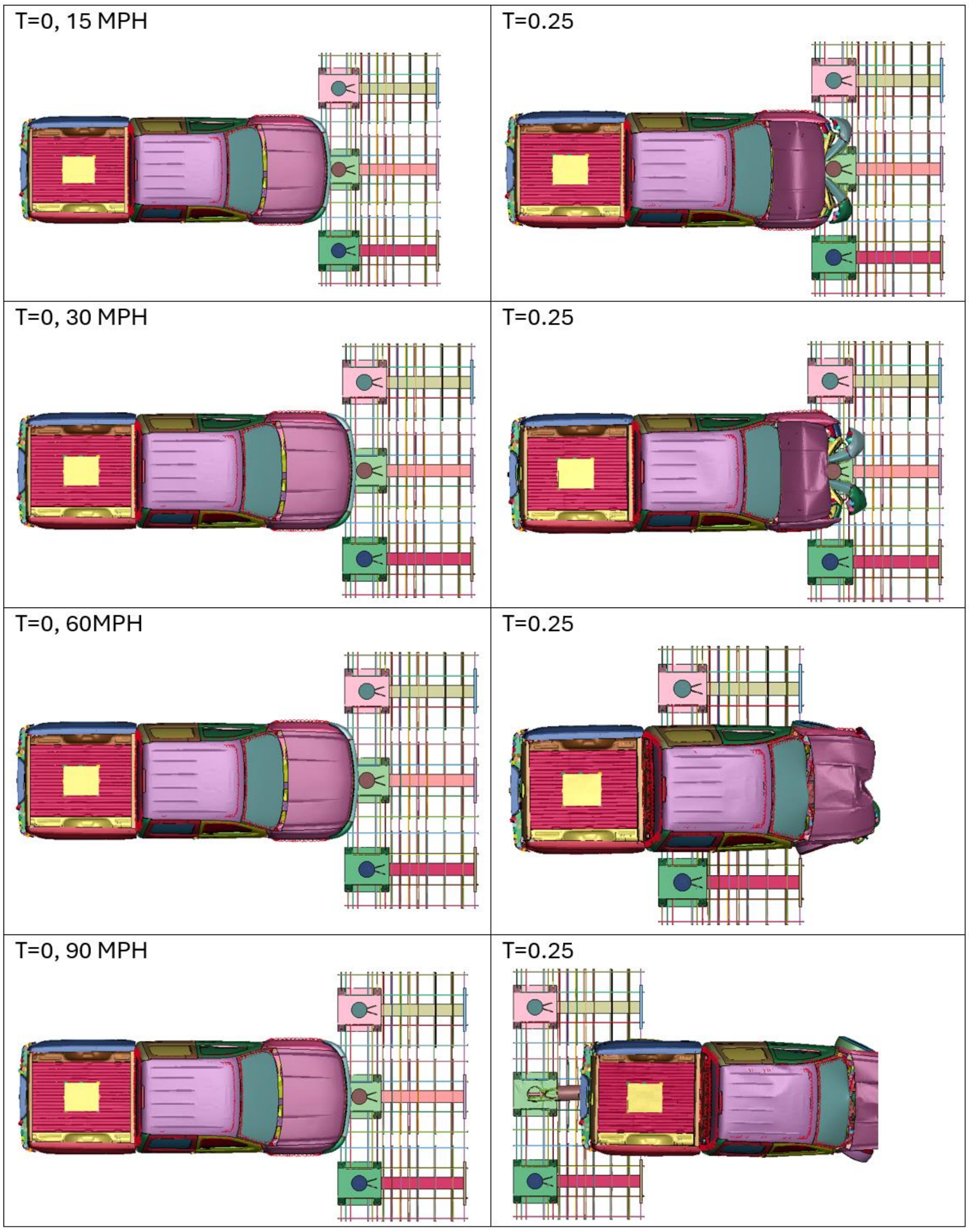

Figure 19. Pre-crash and post-crash images for centered bumper impact at 0° from 15 mph to 90 mph.

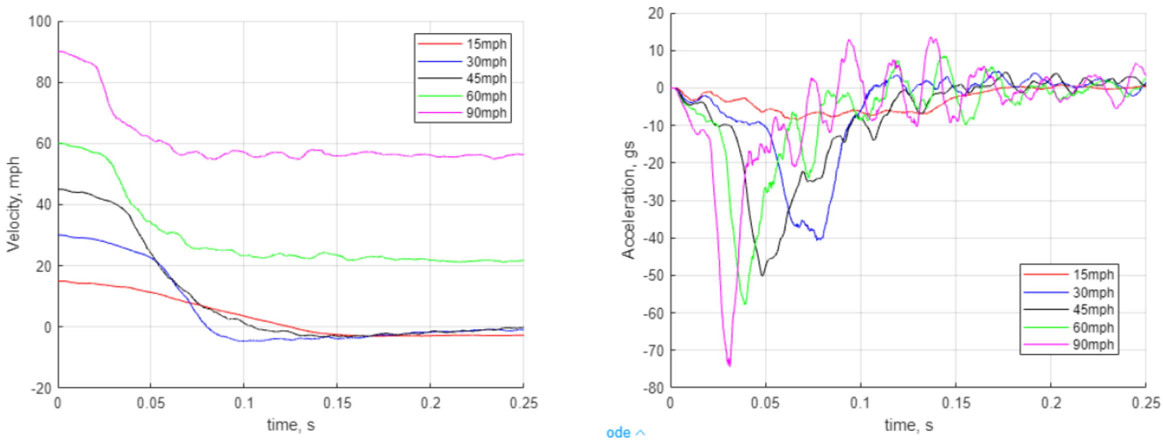

Figure 20. Velocity and acceleration for centered bumper impact at 0° from 15 mph to 90 mph.

The same velocity sweep was simulated with the vehicle impacting the bollard system centered on the bumper at 90°, shown in Figure 21. At 45 MPH or higher, vehicle doesn't stop within 0.25 seconds. And again, higher speeds induce higher peak accelerations upon impact. In this case, due to the impact being along the weak side of the bollard stiffener, the deformation of the bollard causes the vehicle to greatly deform even the second bollard in contact at the 60-mph case.

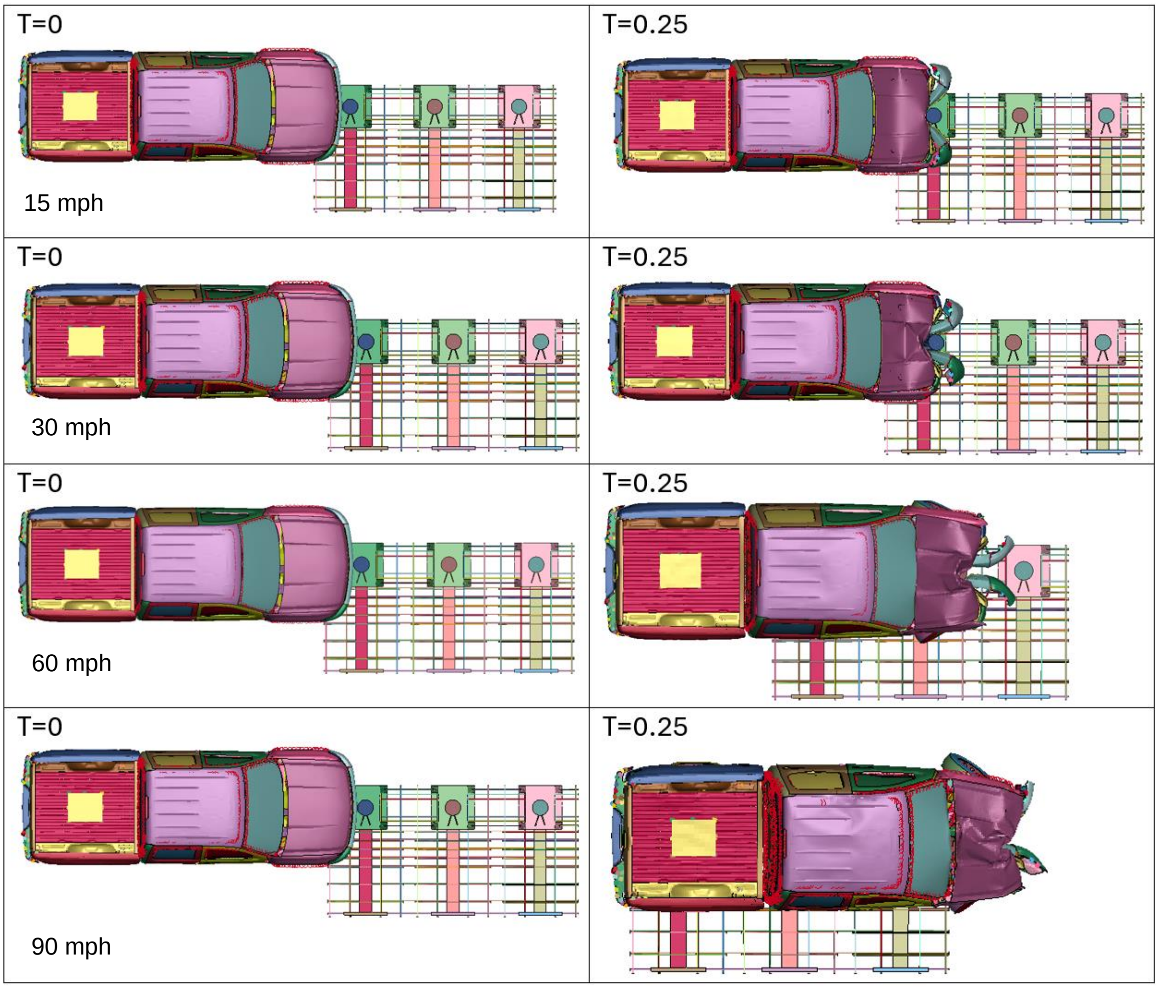

Figure 21. Pre-crash and post-crash images for centered bumper impact at 90° from 15 mph to 90 mph.

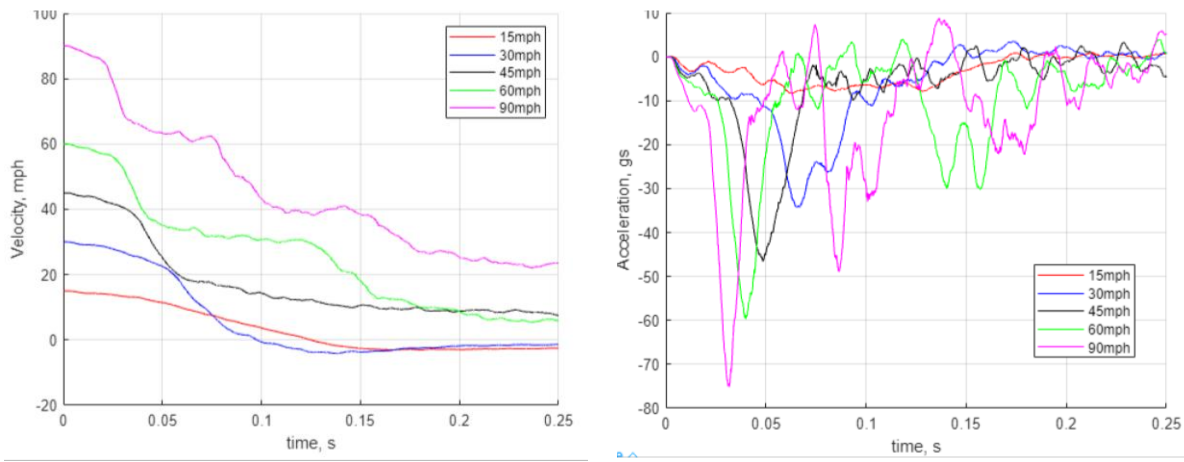

Figure 22. Velocity and acceleration for centered bumper impact at 90° from 15 mph to 90 mph.

6. Conclusions

Overall, the simulations seem to indicate that the current design of the bollard structures used in this application are effective in stopping this type of vehicle traveling at or below 45 MPH, the typical speed limit for many local roads where buses operate. At higher speeds the bollards will slow down but may not effectively stop the vehicle within a reasonable distance. The effectiveness of bollard stopping vehicle is reduced when the vehicle is moving in the street direction. At the worst cases, the first impacted bollard fails completely but other bollards may stop the vehicle.

Off-center impact induces vehicle rotation, which may lead to secondary accidents with another vehicle or pedestrians. At 45 MPH, x-accelerations in the order of 50 g are induced, with slight decrease at higher angles. These acceleration levels can cause severe brain injuries or can be fatal [4].

Additional research on the most probable angles, speeds, and positions of real-world vehicle impacts would greatly improve the scope of this study. This type of data would allow for a narrowing in of parameters to identify the boundaries of effectiveness of the bollard system. Also, though the study primarily looked at the bollard systems ability to stop the vehicle, additional data could be collected and analyzed to see more of the resultant acceleration of various impact conditions to better express the expected passenger experience of the impact. Furthermore, additional research can be conducted to relate the experienced acceleration to human physiological response.

7. References

[1] "Center for Collision Safety and Analysis - 2007 Chevrolet Silverado," Center for Collision Safety and Analysis, December 2016. [Online]. Available: https://www.ccsa.gmu.edu/models/2007-chevrolet-silverado/. [Accessed 28 6 2023].

[2] Regional Transportation Commission of Southern Nevada, "Our Report Card - Ways to Travel," Regional Transportation Commission of Southern Nevada. [Online]. [Accessed 7 6 2022].

[3] E. Marciel, "Bus Stop Bollard Pilot Project," Kimley Horn, Las Vegas, NV, 2020.

[4] C. S. WEAVER, B. K. SLOAN, E. J. BRIZENDINE, and H. BOCK, “An Analysis of Maximum Vehicle G Forces and Brain Injury in Motorsports Crashes,” *Medicine & Science in Sports & Exercise*, vol. 38, no. 2, pp. 246–249, Feb. 2006, doi: https://doi.org/10.1249/01.mss.0000184773.07870.5e.